MOLECULAR ENDOCRINOLOGY

Conformation of the Mineralocorticoid Receptor N-terminal Domain: Evidence for Induced and Stable Structure

Katharina Fischer, Sharon M. Kelly, Kate Watt, Nicholas C. Price and Iain J. McEwan

Mol. Endocrinol. 2010 24:1935-1948 originally published online Aug 4, 2010; , doi: 10.1210/me.2010-0005

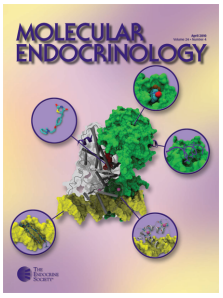

Conformation of the Mineralocorticoid Receptor N-terminal Domain: Evidence for Induced and Stable Structure

Katharina Fischer, Sharon M. Kelly, Kate Watt, Nicholas C. Price, and Iain J. McEwan

Institute of Medical Sciences (K.F., K.W., I.J.M.), University of Aberdeen, Aberdeen AB25 2ZD, Scotland, United Kingdom; and Faculty of Biomedical and Life Sciences (S.M.K., N.C.P.), University of Glasgow, Glasgow G12 8QQ, Scotland, United Kingdom

The mineralocorticoid receptor (MR) binds the steroid hormones aldosterone and cortisol and has an important physiological role in the control of salt homeostasis. Regions of the protein important for gene regulation have been mapped to the amino-terminal domain (NTD) and termed activation function (AF)1a, AF1b, and middle domain (MD). In the present study, we used a combination of biophysical and biochemical techniques to investigate the folding and function of the MR-NTD transactivation functions. We demonstrate that MR-AF1a and MR-MD have relatively little stable secondary structure but have the propensity to form α-helical conformation. Induced folding of the MR-MD enhanced protein-protein binding with a number of coregulatory proteins, including the coactivator cAMP response element-binding protein-binding protein and the corepressors SMRT and RIP140. By contrast, the MR-AF1b domain appeared to have a more stable conformation consisting predominantly of β-secondary structure. Furthermore, MR-AF1b specifically interacted with the TATA-binding protein, via an LxxLL-like motif, in the absence of induced folding. Together, these data suggest that the MR-NTD contains a complex transactivation system made up of distinct structural and functional domains. The results are discussed in the context of the induced folding paradigm for steroid receptor NTDs. **(*Molecular Endocrinology* 151: 1935–1948, 2010)**

NURSA Molecule Pages: Nuclear Receptors: MR; **Coregulators:** GRIP1 | AIB1 | CBP | SMRT | RIP140.

The mineralocorticoid receptor (MR) is a ligand activated transcription factor and member of the steroid hormone receptor (SHR) subfamily of nuclear receptors. With its natural ligand aldosterone, it plays a major role in the regulation of salt homeostasis in epithelial cells of the colon and distal nephron of the kidney. The receptor is also expressed in nonepithelial cells, including cardiomyoctes, neurones, and cells of the vasculature (reviewed in Refs. 1–6). Polymorphisms and point mutations in the receptor are associated with various diseases, including pseudohypoaldosteronism type 1, early on-set hypertension, and cardiac dysfunction (4, 5). SHRs have a well-characterized structural organization consisting of a distinct amino-terminal domain (NTD) important for transactivation of transcription [activation function (AF)1], followed by a DNA-binding domain (DBD), which is important for specific DNA binding and dimerization, a hinge region, and at the carboxy terminus, a ligand-binding domain (LBD) important for hormone binding, protein-protein interactions, and further transactivation activity (AF2) (7, 8). Significantly, the length of the NTD of nuclear receptors has been correlated with the relative importance of the AF1 domain for receptor-dependent transactivation (9). With a total length of 602 amino acids, the MR-NTD is the longest of all members of SHR subfamily (10, 11). Three different parts within the NTD have been identified as being important for re-

Abbreviations: AF, Activation function; AR, androgen receptor; CBP, cAMP response element-binding protein-binding protein; CD, circular dichroism; DBD, DNA-binding domain; ELL, eleven-nineteen lysine-rich leukemia; ER, estrogen receptor; FKBP, FK506 binding protein; GR, glucocorticoid receptor; GRE, glucocorticoid response element; GST, glutathione S-transferase; hMR, human MR; LBD, ligand-binding domain; MD, middle domain; MR, mineralocorticoid receptor; NTD, amino-terminal domain; PIAS, protein inhibitor of activated signal transducer and activator of transcript; PR, progesterone receptor; RHA, RNA helicase A; SDS, sodium dodecyl sulfate; SHR, steroid hormone receptor; SRC, steroid receptor coactivator; TBP, TATA-binding protein; TFE, trifluoroethanol; TMAO, trimethyl N-oxide.

ISSN Print 0888-8809 ISSN Online 1944-9917
Printed in U.S.A.

doi: 10.1210/me.2010-0005 Received January 7, 2010. Accepted July 7, 2010.
First Published Online August 4, 2010

ceptor transactivation. The groups of Kato and co-workers (12) and Lombès and co-workers (13) identified two regions in the human and rat MR-NTD, termed AF1a (amino acids 1-169) and AF1b (amino acids 451-602) that were important for transactivation. By contrast, Govindan and Warriar (14) reported that the central part of the human MR (hMR)-NTD (amino acids 247-385) acted as a transactivation domain. However, an inhibitory function has also been reported for this region (13).

How exactly transcriptional regulation by the MR is distinguished from the most closely related glucocorticoid receptor (GR) is a topic of active research and debate, and the differences are likely to occur at several levels (4, 11, 15, 16). Given the high degree of sequence and structural homology the MR-DBD and LBD share with the GR, it seems likely that a critical region to distinguish the action of both receptors lies within the NTD, which shows only 15% homology (4, 15–20).

Little is known about the MR-NTD with respect to its folding and function. Several coactivators, such as the p160 family protein SRC2 or RNA helicase A (RHA)/cAMP response element-binding protein-binding protein (CBP) complexes have been shown to potentiate the transactivation activity of the AF1b and AF1a domains, respectively (12, 21), but no direct link between structure and function has been made. Studies on AF1 transactivation domains within the NTD of the androgen receptor (AR), GR, estrogen receptor (ER)α, as well as progesterone receptor (PR) have revealed that isolated recombinant proteins are largely unstructured in solution with the potential to form structure, which can be induced in the presence of the natural osmolyte trimethyl N-oxide (TMAO), the hydrophobic solvent trifluoroethanol (TFE), interacting proteins, or other receptor domains, such as the DBD (7, 8, 22–25). An induced folding mechanism for the AR-AF1 upon TFIIF binding (26, 27) and for the GR-AF1 upon interaction with the TATA-binding protein (TBP) (28) and an overall increase in α-helical content for both of the otherwise unstructured transactivation domains has been observed. Further more, binding of AR-AF1 and GR-AF1 domains to coregulatory proteins was increased after folding of the respective domains with TMAO as shown by glutathione S-transferase (GST) pull-down assays (27, 29). Similarly, the unstructured ERα-NTD interacted with TBP and conformed to the model of induced protein folding after binding to TBP (22) and binding of the Jun-dimerization protein 2 to the PR-DBD resulted in folding of the PR-NTD (24).

The fact that the NTD of other members of the SHR subfamily interact with the general transcription factors TBP or TFIIF and undergo structural changes within this domain led to the question of whether the proposed model of induced protein folding is common to all members of this group of transcription factors, including the MR-NTD. According to this paradigm, SHR-NTDs exist in cells in a conformational state, showing significant natural disordered structure and adopt a more folded conformation upon protein-protein interactions when needed to activate transcription (reviewed in Refs. 8, 23, 25). The adopted structure thereby serves as a platform for further protein-protein interactions, leading to a complex that enables transcription initiation. In the present study, we sought to identify novel binding partners for the MR-NTD and determine whether this region harbors AF1 domains that conform to the model of induced protein folding. The data presented show that TBP is a specific binding partner for the AF1b domain, but that binding is not in accordance with the above model of induced folding as shown by circular dichroism (CD) and fluorescence spectroscopy and GST pull-down assays. These data argue for alternative binding interactions of TBP with the relatively structured MR-AF1b domain in contrast to the AF1 of the AR, GR, and ERα. Interestingly, the MR-AF1a and MR-middle domain (MD) transactivation domains do appear to lack stable secondary structure, in the absence of structure-stabilizing agents, and binding of coregulatory proteins to MR-MD was enhanced by prior folding of this domain with the natural osmolyte TMAO. Taken together, the data suggest that the MR-NTD contains a complex transactivation system with structurally and functionally distinct domains.

Results

Expression and purification of MR-AF1a, MR-MD, and MR-AF1b domains

The structural organization of the MR is depicted in Fig. 1A, showing the LBD, DBD, and unique NTD comprising amino acids 1-602. The three regions identified as regulating transcription are highlighted below. MR-AF1a (amino acids 1-169) is predicted to be largely α-helical (47%) and to have regions of intrinsic disorder in the N-terminal half, between amino acids 1 and 107 and a peak at amino acids 121-130 (Fig. 1A). The MR-AF1b domain (amino acids 450-602) has been mapped to the carboxy-terminal part of the NTD and is predicted to be predominantly ordered, with a high proportion of β-strand structure (34%), a segment of disordered structure between amino acids 570 and 602, and a short stretch of unstructured amino acids depicted by a peak around 500-525 (Fig. 1A). The MD (amino acids 247-

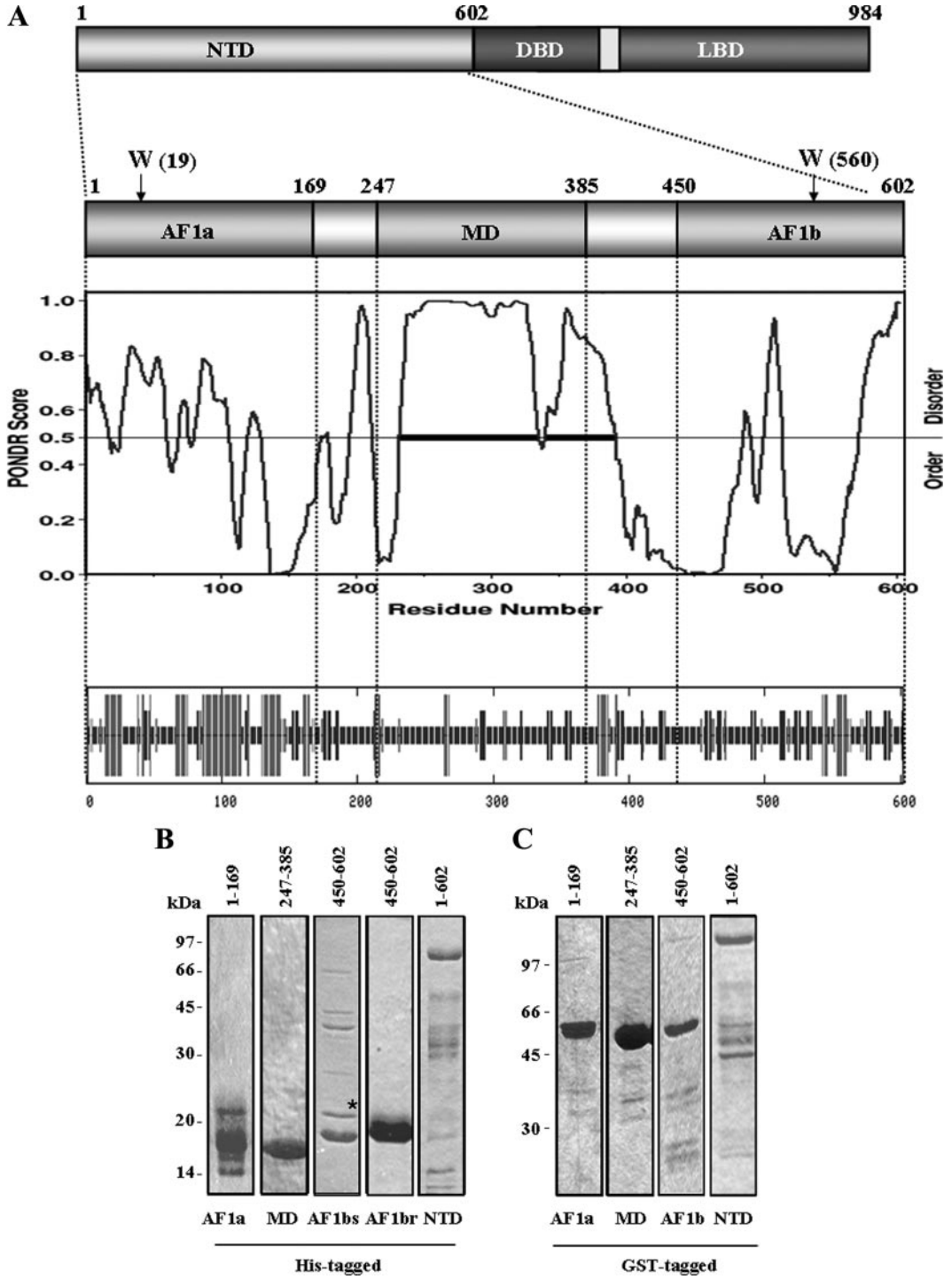

FIG. 1. MR domain organization and purified recombinant proteins. A, Schematic drawing of the hMR showing the domain organization. *Numbers* indicate amino acid positions. *Below* is an enlarged view of the MR-NTD, amino acids 1-602, highlighting the three domains important for MR-dependent gene regulation: AF1a, MD, and AF1b (12–14). The location of two tryptophan (W) residues is also indicated. *Below* are two structure prediction plots: a PONDR plot (56, 57), which is a prediction of natural disordered structure (positive peaks above 0.5), and *below*, the predictions of secondary structure using Network Protein Sequence Analysis (see http://pbil.ibcp.fr/htm/index.php) (58): the *large bars* represent α-helix, *small bars* represent β-strand, and the *middle line* represents nonordered structure. B, Coomassie-stained gel of purified His-tagged MR-AF1a, MR-MD, MR-AF1b polypeptides, and MR-NTD. MR-AF1b was purified from the insoluble (AF1br) or soluble (AF1bs) bacterial fractions. *An asterisk* indicates the copurifying bacterial FKBP type chaperone. The amount of protein loaded was 7.0, 2.0, 4.6, 3.0, and 1.7 μg for MR-AF1a, MR-MD, MR-AF1bs, MR-AF1br, and NTD, respectively. C, Coomassie-stained gel of purified GST-tagged MR-AF1a, MR-MD, AF1b, and NTD polypeptides. The amount of protein loaded was 2.7, 6.0, 1.0, and 2.8 μg for MR-AF1a, MR-MD, MR-AF1b, and MR-NTD, respectively.

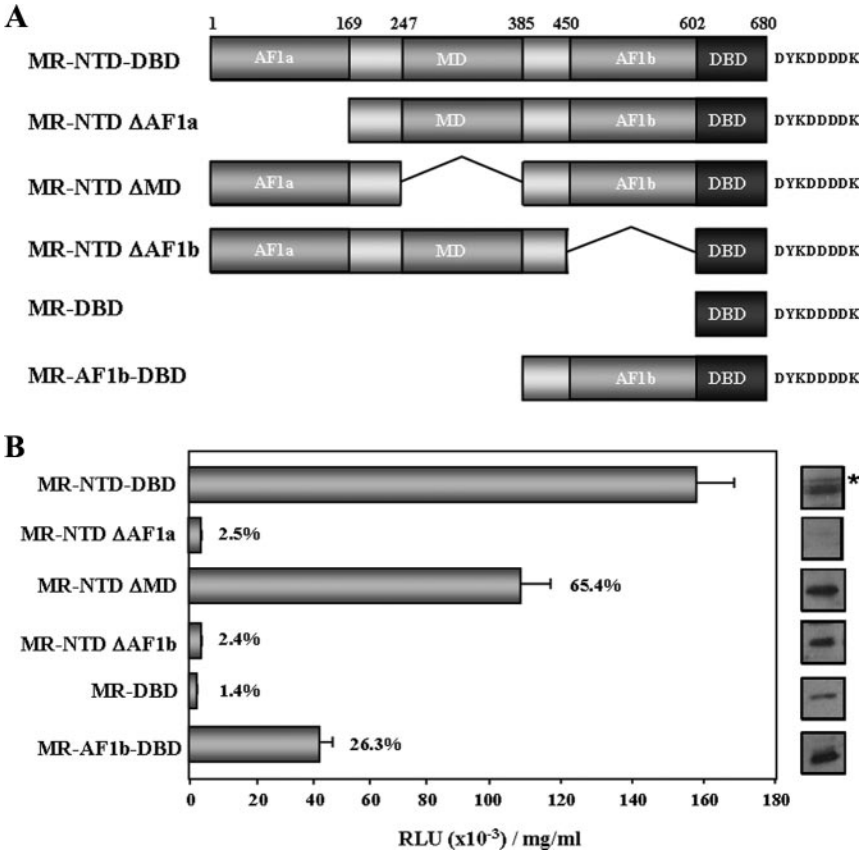

FIG. 2. Reporter gene activity for MR-NTD-DBD and AF1 deletions. A, Schematic representation of the MR-NTD-DBD-FLAG construct and the transactivation domain deletions. B, The wild-type or mutant MR-NTD-DBD constructs were transfected along with a $(GRE)_2$-TATA-luciferase reporter gene into COS-1 cells and transactivation activity measured. Transfections were done in triplicate, and the mean ± SD is shown. On the *right* is shown a Western blot analysis of the expressed proteins detected with an anti-FLAG antibody. *An asterisk* indicates a nonspecific protein detected in some blots. The % activity relative to the wild-type protein (100%) is also shown.

385) is predicted to have little secondary structure (77% random coil) and to be predominantly unstructured (Predictors of Natural Disordered Regions score >0.5 and solid line) (Fig. 1A). Expression constructs for N-terminally His- or GST-tagged MR-NTD polypeptides were generated and recombinant proteins purified as described in *Materials and Methods*. His-tagged MR-AF1b was purified from the insoluble bacterial protein fraction and refolded *in vitro* (AF1br) (Fig. 1B), because under nondenaturing conditions, a second protein copurified with the MR polypeptide, which was identified by mass spectrometry as an *Escherichia coli* FK506 binding protein (FKBP) type chaperone (AF1bs) (Fig. 1B) (data not shown). Concomitant with the elimination of the chaperone, there was a loss of stability of the MR-AF1b polypeptide, purified from the insoluble bacterial fraction. This lack of stability became apparent during refolding as the final dialysis step against buffer lacking urea resulted in protein precipitation. A detergent that has been shown to stabilize β-secondary structure at low concentrations is sodium dodecyl sulfate (SDS) (30, 31), and when added during the last dialysis step at a concentration of 1.7 mM, no signs of precipitation of the His-tagged MR-AF1b was observed. Figure 1, B and C, shows the purified recombinant proteins, which from the stained gel and Image J quantification were estimated to be greater than 90% pure for His-MR-MD, His-MR-AF1br, and GST proteins and 55 to 60% for His-MR-AF1bs, due to the copurification of the bacterial FKBP.

Distinct regions of the MR-NTD contribute to transcriptional activation

To confirm the importance of regions within the NTD for transactivation, a construct was made containing the NTD-DBD with a FLAG tag and transfected into COS-1 cells together with a luciferase reporter gene driven by two glucocorticoid response elements (GREs). Figure 2A shows the MR-NTD-DBD polypeptide and a series of deletion mutant proteins. Deletion of the MD reduced the transcriptional activity of the NTD by 35%, whereas deleting AF1a or AF1b region resulted in a loss of greater than 97% of the activity of the full NTD (Fig. 2B). Importantly, the AF1b domain alone linked to the DBD retained 26% the activity of the MR-NTD-DBD polypeptide (Fig. 1B). The wild-type and deletion proteins were all expressed at similar levels, with the exception of MR-ΔAF1a. Thus, the loss of transactivation activity with this construct, in the present study, may be a consequence of inefficient translation or increased degradation. However, overall, these data are in good agreement with published work on the MR-AF1 transactivation function.

Conformational analysis of the MR-AF1a, MR-MD, and MR-AF1b domains

Measuring the steady-state fluorescence emission spectrum for a protein is a useful method for monitoring the local tertiary structure surrounding aromatic amino acids and the folding/unfolding of the polypeptide in different environments. MR-AF1a and MR-AF1b both contain a single tryptophan residue, amino acids 19 and 560, respectively, and 5 or 8 tyrosine residues, respectively. The emission spectrum for tryptophan is sensitive to changes

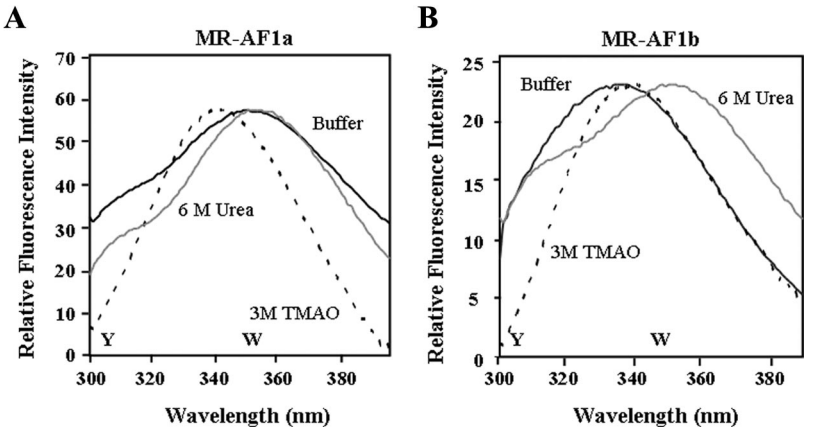

FIG. 3. Steady-state fluorescence emission spectra for MR-AF1a and MR-AF1b. A and B, The steady-state fluorescence emission spectra for His-tagged MR-AF1a and MR-AF1br, respectively, in either phosphate buffer (*black line*), 6 M urea (*gray line*), or 3 M TMAO (*broken line*) after excitation at 278 nm. The data are a representative experiment, and the results of at least three independent experiments showing the mean value ± SD are summarized in Table 1. W and Y represent the emission wavelength for tryptophan and tyrosine, respectively, for the proteins in buffer.

in polarity upon exposure to solvent, whereas the emission from tyrosine residues will be quenched by any tryptophan residues in close proximity (32). After excitation at 278 nm, MR-AF1a and MR-AF1b showed distinct emission spectra (Fig. 3). The tryptophan in MR-AF1a is essentially solvent exposed with a λ_{max} of 351 nm, *i.e.* not significantly changed by urea-induced unfolding (Fig. 3A and Table 1). In the presence of the osmolyte TMAO, a natural solute that stabilizes native structure (33), there is a clear "blue shift" of the λ_{max} to 341 nm consistent with the tryptophan residue becoming less solvent exposed. MR-AF1a was also sensitive to rapid limited trypsin digestion in the absence of TMAO, resulting in a doublet of fragments between 14 and 20 kDa, which lack sequences from the N terminus (Supplemental Fig. 1A, published on The Endocrine Society's Journals Online web site at http://mend.endojournals.org). By contrast, the spectrum for MR-AF1b in buffer suggests that the tryptophan is shielded from aqueous solvent already in buffer and there is no further change in the presence of TMAO (Fig. 3B and Table 1). However, after urea-induced unfolding, there was a distinct "red shift" of the λ_{max} to 347 nm, indicating that the tryptophan residue is becoming more solvent exposed. Taken together, these results are consistent with the MR-AF1b domain being stably folded, whereas the MR-AF1a can undergo induced folding in the presence of TMAO.

Given that the MR-AF1b polypeptide purified from inclusion bodies requires low concentrations of SDS for its stability, we addressed the question of the conformation of this domain from the soluble fraction under the same buffer conditions. The λ_{max} values for tryptophan emission are summarized in Table 1. The results were essentially the same as for the refolded polypeptide, with the tryptophan residue buried in buffer, but becoming more solvent exposed after urea-induced unfolding. To investigate the conformation of MR-AF1br in SDS in more detail, the polypeptide was challenged with the protease trypsin and the products of a partial proteolytic digest analyzed over time. Although there are 10 predicted trypsin cleavage sites within the MR-AF1b, this domain was significantly resistant to proteolytic digestion with a dominant series of fragments, between 14 and 20 kDa, generated after 20 min, which were identified as retaining amino terminal regions of AF1b by Western blot analysis (Supplemental Fig. 1C). Even after a 60-min incubation, there was significant levels of full-length MR-AF1b remaining (Supplemental Fig. 1C, *filled arrowheads*). This would be consistent with the structure predictions shown in Fig. 1B. Resistance to proteolytic cleavage was not due to the inhibition of trypsin activity by SDS, because the rates of cleavage of the artificial trypsin substrate N-α-benzoyl-L-arginine ethyl ester were identical in the presence or absence of SDS (Supplemental Fig. 1D).

In the absence of tryptophan residues, the conformation of the MR-MD polypeptide was investigated by limited proteolysis. Supplemental Fig. 1B shows that the MR-MD polypeptide is digested in a time-dependent manner, and this digestion is prevented in the presence of TMAO. This is consistent with induced folding of the MD and adoption of a more protease-resistant conformation. Previously, we and others have shown that TMAO does not inhibit protease activity (34). Collectively, the data

TABLE 1. Summary of steady-state fluorescence spectroscopy data

	Mean λ_{max} ± SD (nm)				
Protein	**Buffer**	**TMAO**	**Urea**	**Δλ blue shift**	**Δλ red shift**
AF1a	351 ± 2	341 ± 1	353 ± 2	10 nm	2 nm
AF1br	336 ± 3	338 ± 3	347 ± 3	—	9 nm
AF1bs	339 ± 1	337 ± 3	345 ± 2	2 nm	7 nm
NTD	347 ± 2	340 ± 3	351 ± 2	7 nm	4 nm

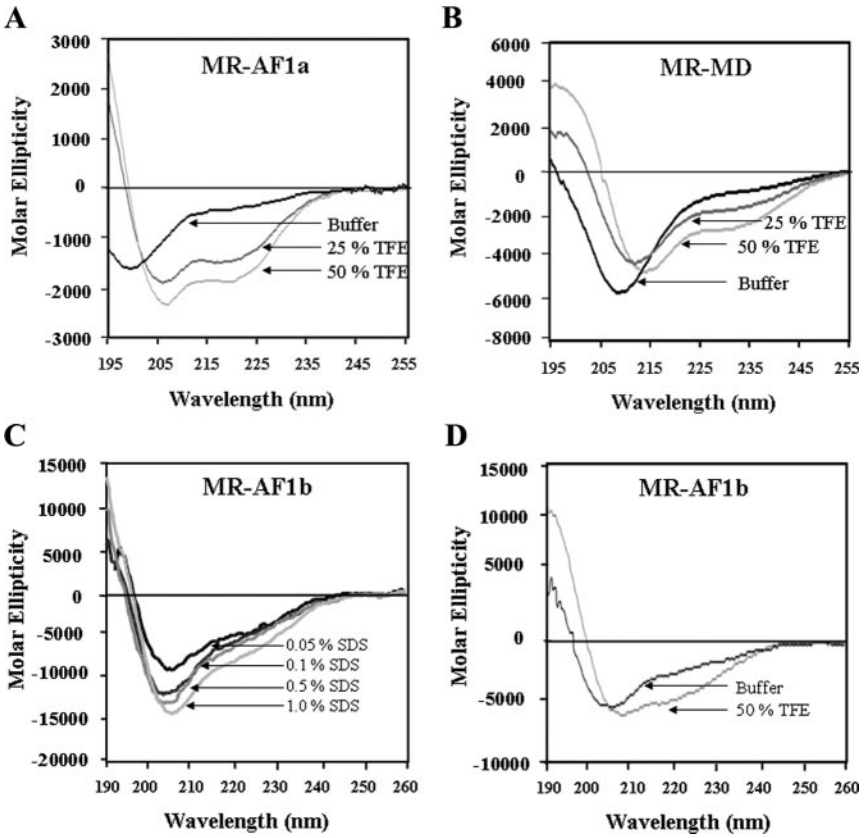

FIG. 4. Secondary structure analysis of the MR-NTD transactivation functions. A and B, Far-UV CD spectra for the MR-AF1a and MR-MD domains, at concentrations of 0.5–0.8 mg/ml, recorded in buffer (*black line*) or 25 or 50% TFE (*gray lines*). Estimates of secondary structure are summarized in Table 2. C, Far-UV CD spectra for the MR-AF1br, at concentrations in the range from 0.07 to 0.2 mg/ml, were recorded in increasing concentrations of SDS. Spectra are characteristic for a mixed α/β protein, with primarily β-secondary structure as summarized in Table 2. D, As for C, except 50% TFE was included in buffer (*gray line*).

suggest that the MR-AF1b is a stably folded polypeptide in the presence of low concentrations of SDS, whereas MR-AF1a and MR-MD are less stably folded in the absence of the osmolyte TMAO.

MR-AF1a and MR-MD polypeptides have the propensity to form α-helical conformation, whereas MR-AF1b adopts a predominantly β-secondary structure

Far-UV CD analysis can be used to determine secondary structure elements of proteins by observing spectra resulting from conformational states of peptide bonds within proteins. We investigated the secondary structure content of the three MR-NTD domains associated with transactivation. Figure 4A shows the far-UV spectrum for MR-AF1a in buffer and with increasing amounts of the hydrophobic solvent TFE, which has been widely used as an experimental tool to stabilize secondary structure. The spectrum in buffer shows a strong minimum at around 197 nm, which is indicative of nonordered structure (Fig. 4A). In contrast, in the presence of increasing amounts of TFE, there is increasing negative ellipticity at 209 and at 222 nm, which is associated with an increase in α-helical content at the expense of both β-structure and nonordered structure (Fig. 4A and Table 2). The far-UV spectra for MR-MD showed a similar trend with a more helical conformation adopted in the presence of TFE (Fig. 4B and Table 2). TMAO was not used in these studies, because it shows strong absorption at low wavelengths that interferes with the recording and analysis of the CD spectrum.

In 1981, Wu *et al.* (30) carried out extensive CD studies on the effect of SDS on protein structure. They concluded that proteins with β-structure-forming potential can adopt this structure in the presence of low concentrations of SDS (2 mM), but at higher concentrations (25 mM), a partial β-sheet to helix transition can be observed. We investigated whether the AF1b adopts primarily β-structure at the low concentrations of SDS used (1.7 mM/0.05%) and whether the sheet to helix conformational changes could be observed at higher concentrations (up to 34 mM/1.0%) of detergent. Solutions of approximately 0.1 mg/ml of highly purified AF1b were used to record far-UV CD spectra at increasing concentrations of SDS (Fig. 4C). With a positive ellipticity below 200 nm and negative ellipticity between 200 and 240 nm, the spectrum of this protein is in accordance with

TABLE 2. Summary of CD data for MR-NTD transactivation system

	Secondary structure				
	α-Helix	β-Strand	β-Turn	RC	Total
AF1a buffer	11	29	25	36	101
AF1a 50% TFE	63	5	10	22	100
MD buffer	13	22	24	40	99
MD 50% TFE	66	13	7	15	101
AF1b (0.05% SDS) buffer	19	32	31	19	101
AF1b 50% TFE	13	31	23	33	100
AF1b 0.1% SDS	18	25	26	31	100
AF1b 0.5% SDS	16	27	24	33	100
AF1b 1.0% SDS	19	26	25	30	100
NTD buffer	20	21	24	35	100
NTD 50% TFE	79	2	3	15	99

Secondary structure determinations (in %) as estimated by the CDSSTR procedure [Sreerama and Woody (55)]. RC, Random coil.

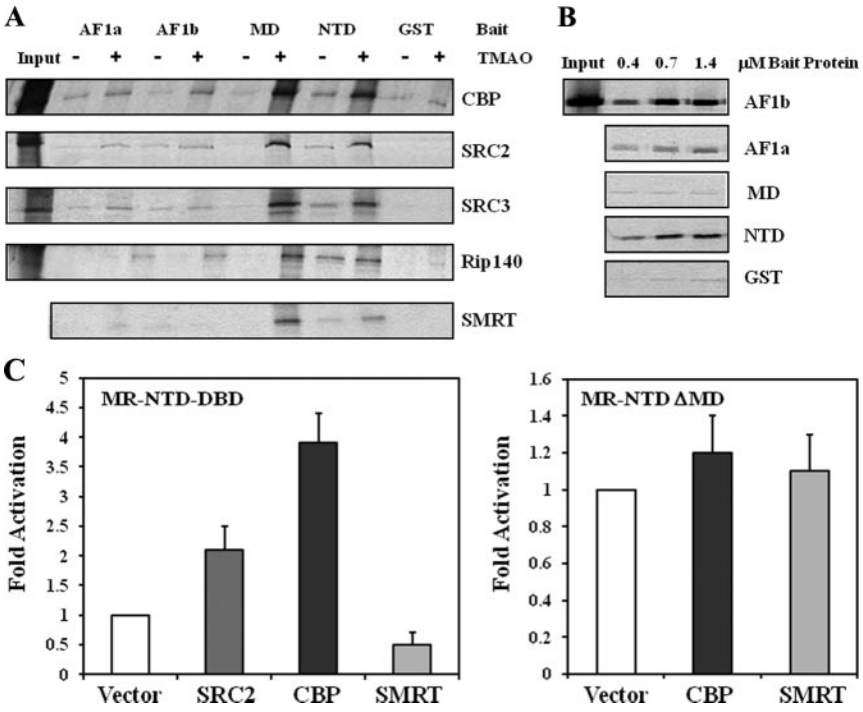

FIG. 5. *In vitro* protein-protein interactions. A, GST pull-down assays were performed with 0.7 μM bait protein (GST, GST-MR-NTD, GST-MR-AF1a, GST-MR-MD, or GST-MR-AF1b) and *in vitro* synthesized and radiolabeled coactivators (SRC2, SRC3, and CBP) and corepressors (SMRT and Rip140). Experiments were done in the absence (−) or presence (+) of 3 M TMAO. The results are representative of at least two independent experiments; 10% of the input labeled protein is indicated. B, A representative experiment showing binding of the general transcription factor TBP to increasing concentrations of GST alone or GST-MR polypeptides. Preferential binding to AF1b and NTD was observed in the absence of TMAO. Quantitation of the gels shown was as follows: AF1b: 4, 28, and 29 arbitrary units; NTD: 10.6, 16.8, and 20.8 arbitrary units; and AF1a: 1, 5.3, and 6.9 arbitrary units, respectively. C, The wild-type (MR-NTD-DBD) or mutant (MR-NTD-ΔMD-DBD) constructs were transfected along with a $(GRE)_2$-TATA-luciferase reporter gene into COS-1 cells, with or without the coregulatory proteins CBP, SRC2, or SMRT and transactivation activity measured. Transfections were done in duplicate or triplicate, and the mean fold activation ± SD is shown for one or two experiments.

a spectrum resulting from a mixed α/β protein. The spectrum for the MR-AF1b domain revealed significant β-strand and turn elements comprising a total of 63% all together in 1.7 mM SDS with only 19% α-helical content (Fig. 4C and Table 2). An overall decrease in β-structure with increasing amounts of SDS (up to 34 mM) could be observed with concomitant increase in random coil, but not α-helix, which indicates that no induced α-helical structure is formed at higher concentrations of SDS (Fig. 4C and Table 2). Interestingly, in the presence of 50% TFE, there was again a general increase in random coil (Fig. 4D and Table 2), which is in contrast to the effects of this hydrophobic solvent on the MR-AF1a and MR-MD domains and the published studies for the AR-AF1 (26) and GR-AF1 (35), where a significant increase in α-helical structure was observed. Although TFE has generally been shown to induce α-helix, it has also been shown to stabilize β-strands, and hence its action seem to depend on the nature of the protein involved and its structure-forming potential (31). Overall, the results are in accordance with the structure predictions that the MR-AF1b adopts β-secondary structure and has little propensity, unlike MR-AF1a and MR-MD, to form significant amounts of α-helix.

Conformational analysis of the full-length MR-NTD

Fluorescence and far-UV spectroscopy analysis of the full-length MR-NTD revealed some composite structural properties seen with the isolated domains, but generally, the fluorescence emission for the solvent exposed tryptophan was dominant, and the polypeptide showed a propensity to form helical secondary structure in a hydrophobic environment (Tables 1 and 2 and Supplemental Fig. 2, A and B). Strikingly, when the NTD is digested with trypsin in the absence of TMAO, two prominent fragments are observed, which are not recognized by the antihistidine antibody (Supplemental Fig. 2C). From the lack of N-terminal sequences and the size of these fragments, it is tempting to speculate that they represent the protease resistant AF1b domain.

Multiple protein-protein interactions with distinct regions of the MR-NTD

Relatively few direct protein-binding partners for the MR-NTD have been identified or characterized to date. Using an *in vitro* protein-protein interaction assay, we screened panels of known general transcription factors, coactivators, and corepressor proteins for binding to MR-NTD or the isolated transactivation domains. Figure 5 shows representative results for GST pull-down assays. Figure 5A shows the selective binding of members of the p160 coactivator family, steroid receptor coactivator (SRC)2 and SCR3, and the CBP to the MR-MD and the MR-NTD, but only after induced folding or stabilization of conformation by TMAO (+). Importantly, TMAO did not significantly increase binding of any of these factors to the MR-AF1a or MR-AF1b domains or GST alone, indicating the interactions were specific for the folded MD. Similarly, binding of corepressor proteins, SMRT and RIP140, was specific for the MR-MD and MR-NTD after TMAO treatment (Fig. 5A). Again there was no significant binding to either MR-AF1a or MR-AF1b coactivator proteins, irrespective of

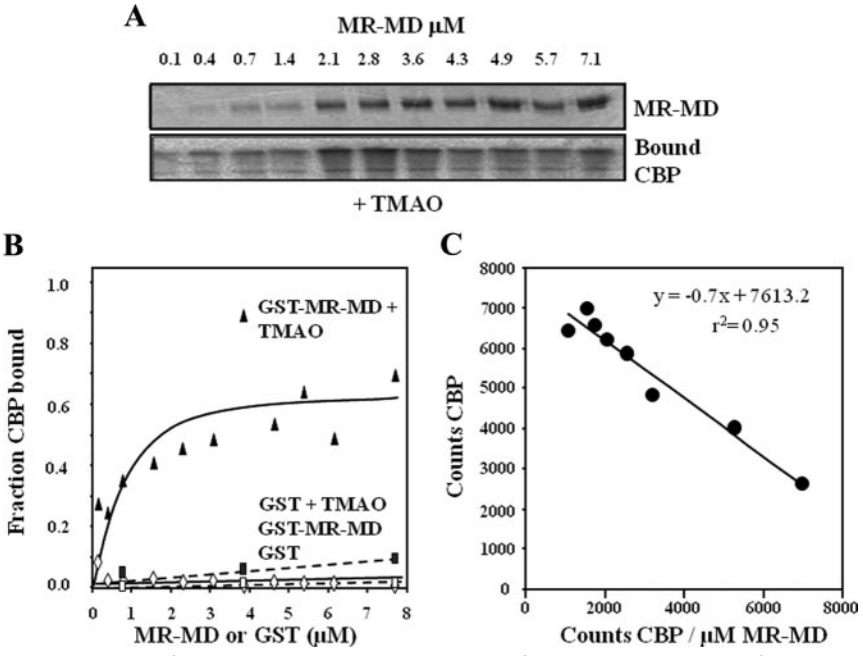

FIG. 6. Binding of CBP to the MR-MD in the presence of TMAO. A, The binding of CBP was measured in the presence of increasing concentrations of GST alone (not shown) or GST-MR-MD in the absence (not shown) or presence of TMAO (+). Bound CBP was analyzed after SDS-PAGE and exposure of the dried gel to a phosphoimaging plate and visualized by AIDA software as depicted (Bound CBP). B, Bound CBP (A) was quantified using AIDA software and plotted as fraction of CBP bound *vs.* concentration of GST (*squares*) or GST-MR-MD (*triangles*) (μM) ± TMAO (*filled* or *open symbols*). The result represents the pooled data from two independent experiments. C, A Eadie-Hofstee plot of the binding data in the presence of TMAO shown in B, from which the dissociation constant, K_d, was calculated.

the presence or absence of TMAO (Fig. 5). By contrast, the TBP was found to preferentially interact with the MR-AF1b domain, and full-length NTD, in the absence of TMAO (Fig. 5B). No selective interactions were indentified for the MR-AF1a domain for any of the proteins tested, although some modest binding of TBP was seen in some experiments (Fig. 5).

In cotransfection experiments, full length, SRC2 and CBP enhanced transactivation by MR-NTD-DBD by 2- and 4-fold, respectively (Fig. 5C, *left panel*). In contrast, cotransfection of SMRT resulted in a 50% decrease in transactivation activity of the MR-NTD (Fig. 5C, *left panel*). Deletion of the MR-MD ablated the coactivation by CBP and the corepression activity of SMRT (Fig. 5C, *right panel*). Collectively, the data from protein-protein interaction assays and cell reporter gene studies reveal that the MR-NTD binds multiple protein targets that may enhance or repress transactivation activity.

The interaction of CBP and TBP with the MR-MD and MR-AF1b domains, respectively, were characterized further using GST pull-down titrations. Figure 6, A and B, shows the binding of radiolabeled CBP binding to the MR-MD. In the absence of TMAO, no specific binding was observed to the MR-MD, or GST, as shown above (Fig. 5). However, in the presence of 3 M TMAO, there was a concentration-dependent increase in binding, which was saturable for the CBP interaction with MR-MD (Fig. 6, A and B). From the curves generated and the corresponding Eadie-Hofstee plot, a dissociation constant of 0.7 μM was calculated for this interaction, as described in the *Materials and Methods* (Fig. 6C). A similar analysis of the interaction of TBP with increasing amounts of GST alone or GST-MR-AF1b, but in the absence of TMAO, also resulted in saturable binding, and from the corresponding Eadie-Hofstee plot, a dissociation constant of 1.4 μM was calculated for this interaction (Fig. 7, A–C).

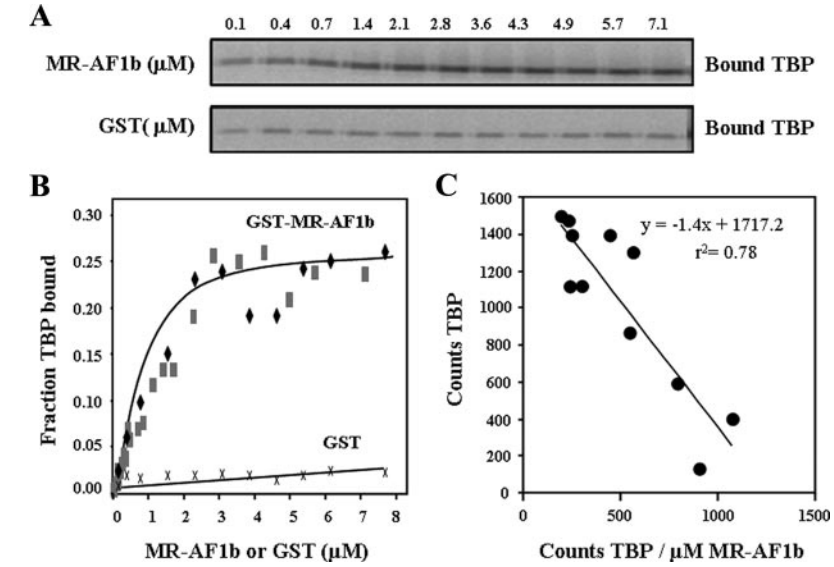

FIG. 7. Binding of TBP to the MR-AF1b domain. A, The binding of TBP was measured in the presence of increasing concentrations of GST alone or GST-MR-AF1b. Bound TBP was analyzed after SDS-PAGE and exposure of the dried gel to a phosphoimaging plate and visualized by AIDA software as depicted. B, Bound TBP (A) was quantified using AIDA software and plotted as fraction of TBP bound *vs.* concentration of GST (x) or GST-MR-AF1b (*filled squares/diamonds*). Two independent titrations are plotted for the binding to MR-AF1b, and the results are representative of at least three independent experiments. C, A linear Eadie-Hofstee plot of the binding data in the presence of TMAO shown in B, from which the dissociation constant, K_d, was calculated.

Binding of TBP to MR-AF1b is mediated by residues within a LxxLL-like motif

Given that the structural properties of the MR-AF1b mediating the interac-

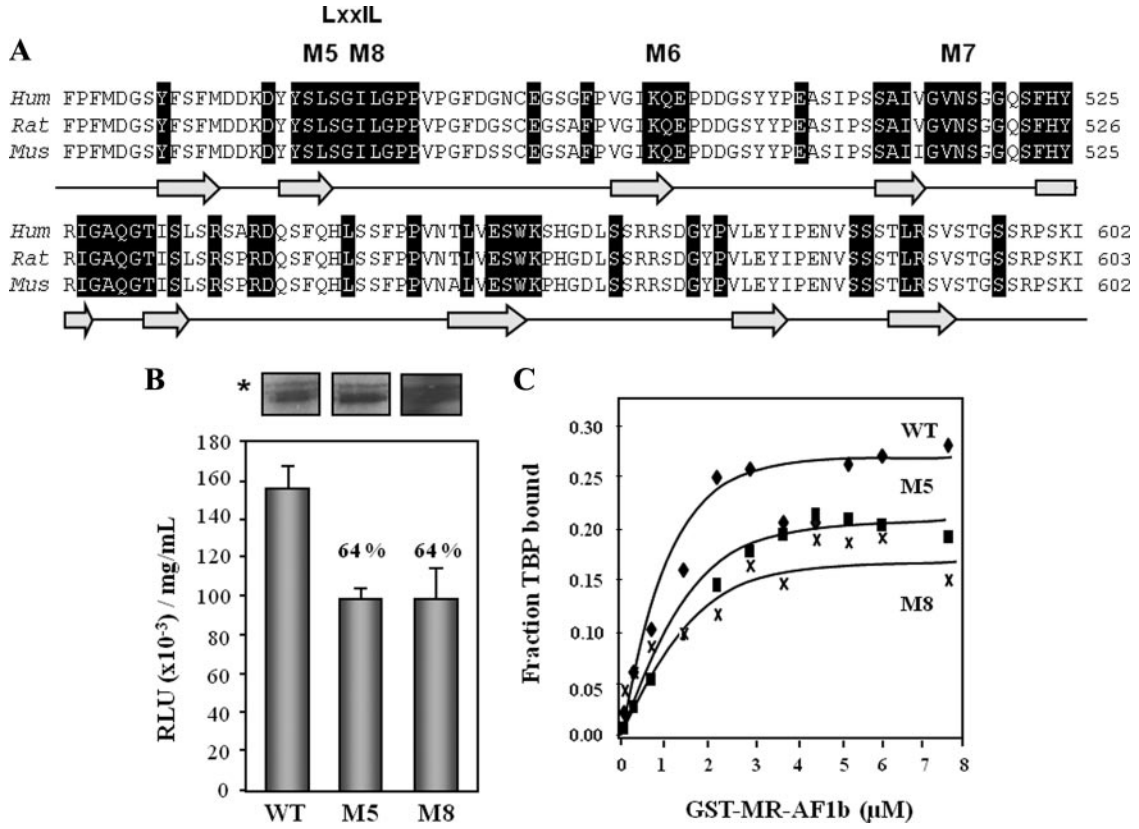

FIG. 8. Mutation of polar and hydrophobic amino acids impair transactivation and TBP binding. A, Primary amino acid sequence alignment of the MR-AF1b domain from human, rat, and mouse; up to 10 additional species were included in the full analysis, including the receptor sequence from *Xenopus* and several fish species. *Black* represents residues conserved in all species studied. The *boxes* represent three triple mutations M5 (S468A, L469A, and S470A), M6 (K497A, Q495A, and E496A), and M7 (V516A, N517A, and S518A), which were introduced into MR-NTD or MR-AF1b. A single point mutation, M8 (L489A), is also indicated. Secondary structure predictions are shown *below the sequence alignment*: *arrows* represent β-strand, and the *lines* represent random coil. B, The mutant or wild-type MR-NTD-DBD-FLAG constructs were transfected into COS-1 cells together with the $(GRE)_2$-TATA-luciferase reporter gene and transactivation activity measured. Transfections were done in triplicate, and the mean ± SD is shown. *Above* is shown a Western blot analysis of the expressed proteins detected with a anti-FLAG antibody. An *asterisk* indicates a nonspecific protein detected in blots for the MR-NTD-FLAG constructs. The % activity relative to the wild-type protein (100%) is also shown. C, The binding of TBP was measured in the presence of increasing concentrations of GST alone or GST-MR-AF1b wild-type (*filled diamonds*) or the M5 (*filled squares*) and M8 (x) mutant polypeptides. Bound TBP was quantified using AIDA software and plotted as fraction of TBP bound *vs.* concentration of GST-MR-AF1b polypeptide (μM). An estimate of the dissociation constant, K_d, for the different MR-AF1b-TBP binding interactions was calculated as described in the legends to Figs. 6 and 7 and the results summarized in Table 3. The data for M5 are from a single experiment, whereas the data for M8 are representative of two independent experiments.

tion with TBP appear distinct from those described for the GR-AF1 (28, 29) and the binding of CBP to MR-MD, we investigated the binding interface in more detail. Comparison of the amino acid sequence of the MR-AF1b domain from different species revealed clusters of highly conserved amino acids (Fig. 8A) (data not shown). A series of triple or single mutations were introduced into AF1b at these conserved residues, in the context of MR-NTD-DBD and the isolated domain (MR-AF1b) (Fig. 8A and Supplemental Fig. 3). Mutating two serine residues and a leucine at positions 468, 469, and 470 (M5) (Fig. 8A) was predicted to disrupt local β-structure and increase α-helix. Mutating these residues or the leucine alone at 469 (M8) (Fig. 8A) impaired transactivation activity in the context of MR-NTD-DBD (Fig. 8B). Mutations introduced into other conserved residues at positions 494, 495, and 496 (M6), 516, 517, and 518 (M7), or single point mutations at I672A (M9) and A512G (M10) also reduced transactivation activity by 30–35% (Supplemental Fig. 3). This reduction in activity is unlikely to be due to changes in receptor levels, because all the mutant polypeptides were expressed to a similar level as the wild-type protein (Fig. 8B and Supplemental Fig. 3). Interestingly, the M5 and M8 mutations also disrupted the binding of TBP, resulting in reduced binding and a 2- to 3-fold reduction in binding affinity (Fig. 8C and Table 3). The effect of the triple (M5) or single (M8) mutations on TBP binding and activity is not due to gross changes in conformation. The λ_{max} for tryptophan fluorescence emission was 339 and 338 nm for M5 and M8, respectively, and was not significantly different from the wild-type protein (336 nm) (Fig. 9A), and both the wild-type and M5 mutant polypeptides showed similar protease sensitivity (Fig. 9B). Taken together, the results of mutational

TABLE 3. TBP binding to MR-AF1b mutations

Protein	Mutation	Activity[a]	K_d[b]
MR-AF1b	WT	100%	1.4 μM
M5	S468A, L469A, S470A	64%	4.6 μM
M8	L469A	64%	2.9 μM

WT, Wild type; K_d, dissociation constant.

[a] Reporter gene assay using MR-NTD-DBD-FLAG.

[b] Binding affinity determined from a representative GST pull-down assays (Figs. 7 and 8) or a single titration experiment in the case of M5.

studies suggest that residues next to or within a highly conserved LxxIL motif in MR-AF1b are important for both transactivation and TBP binding. LxxLL motifs in coregulatory proteins have previously been shown to be important for ligand-dependent binding to a hydrophobic pocket on the surface of the LBD (36).

Discussion

The MR-NTD contains a modular transactivation system, involving discrete regions of the protein. In the present study, we have characterized the structural and functional properties of these regions. The full-length MR-NTD and the isolated MR-AF1a and MR-MD polypeptides appear to have little stable secondary structure in aqueous buffer, but have the propensity to form α-helical conformation in a hydrophobic environment. Further, a solvent-exposed single tryptophan within AF1a underwent a significant blue shift in the presence of the natural osmolyte TMAO, and this domain adopted a more protease resistant conformation. This is indicative of the local environment becoming less solvent exposed and is consistent with induced folding of this domain. Similarly, the MR-MD, which lacks tryptophan residues, adopted a more protease-resistant conformation in the presence of TMAO consistent with induced or stabilized folding. By contrast, MR-AF1b appears to adopt a stable, primarily, β-structure in aqueous buffer and showed little propensity to form α-helix in the presence of high concentrations of either SDS or TFE. Figure 10 summarizes the structural properties of the MR-NTD and the isolated domains.

Using *in vitro* protein-protein interaction assays with GST-tagged proteins, a number of direct binding partners were identified for the MR-MD. These binding interactions included both coactivators and corepressors, but significantly binding was only observed after folding of this domain or the full-length NTD with TMAO. Critically, TMAO treatment did not significantly increase the binding of any of the target proteins tested to either MR-AF1a or MR-AF1b domains. The MR-MD has been proposed to act either positively or negatively in gene regulation (13, 14), which would be consistent with interactions with both coactivators and corepressors. The exact function of this domain may depend on cellular or gene context, and the observed structural plasticity would be advantageous for forming multiple specific protein-protein interactions with modest affinities.

A relatively modest number of coregulatory proteins has been identified that modulates MR-dependent transactivation (see Refs. 5 and 8 and references therein). Members of the p160 coactivator family have been shown to potentiate MR-NTD-dependent transactivation, but no direct interactions were reported (12, 37). Protein-protein interactions with the MR-NTD have been investigated by two-hybrid analysis, GST pull-downs, and chromatin immunoprecipitation assays, and direct binding has been observed for RHA (21), the corepressor DAXX (38), as well as the SUMO-1 E2 conjugating enzyme ubc9 (39) and the E3 ligases, protein inhibitor of activated signal transducer and activator of transcript (PIAS) 1 and PIAS xβ (13) and the elongation factor eleven-nineteen lysine-rich leukemia (ELL) protein (40). ELL enhanced MR transactivation activity and the interaction is particularly interesting, because the binding was mapped in part to the AF1b region (40). RHA was shown to bind directly to the MR-AF1a domain and to form a trimeric complex with CBP (21). In the present study, we show that CBP, and p160 proteins, can bind directly to the MR-MD and result in enhanced transactivation by the MR-NTD. However, none of the coregulatory proteins

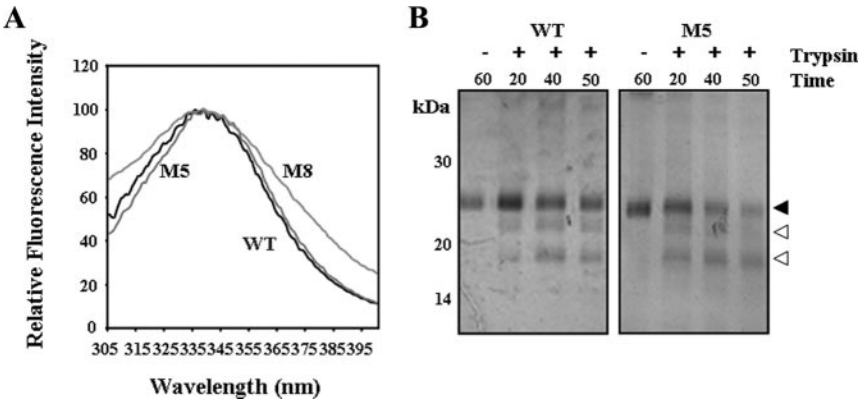

FIG. 9. Mutating residues in a LxxIL motif does not alter gross structure. A, The steady-state fluorescence spectra for wild-type (WT) and M5 AF1br polypeptides are shown. The λ_{max} for tryptophan emission was similar for all three proteins (WT, 336 nm; M5, 339 nm; and M8, 338 nm). B, Limited proteolysis of wild-type and M5 MR-AF1b. The polypeptides were digested with trypsin for the time points indicated and the fragments resolved by SDS-PAGE and detected by Coomassie staining. The pattern of fragments generated (*open arrow heads*) was essentially identical for both polypeptides.

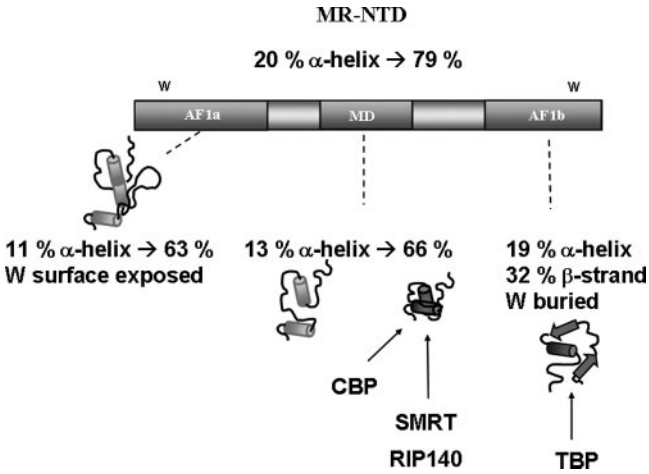

FIG. 10. Summary of the structural and functional properties of the modular MR-NTD transactivation function. Schematic drawing of the MR-NTD showing the three transactivation domains and the position of two tryptophan residues (W). Selected secondary structure content is summarized, and induced folding in the presence of TMAO or TFE is indicated by an *arrowhead* and the *solid cylinders* and *arrows*. The binding of coregulatory proteins to MR-MD and MR-AF1b is also shown.

tested showed preferential binding to MR-AF1a domain in either the presence or absence of the structure stabilizing osmolyte TMAO, although this domain showed similar structural properties of induced folding as MR-MD.

TBP was observed to specifically interact with MR-AF1b with an apparent binding affinity of 1.4 μM. A similar binding affinity, in the range 1-10 μM, has been reported for the binding of TBP to the ERα-NTD (22), but 5- to 9-fold higher affinities were observed for TBP binding to the GR-AF1 (0.19 and 0.25 μM) (41) and the Gal4 transactivation domain (0.16 μM) (42). A model for coupled protein-protein binding and induced folding based on binding kinetics has been proposed by Wright and co-workers (43, 44). They have argued for a two-stage binding reaction, with an initial fast step mediated by electrostatic interactions and a subsequent slower step involving hydrophobic interactions and induced folding. It is interesting, therefore, that the binding of TBP to MR-AF1b, although not requiring induced folding, was modulated by mutating both polar and nonpolar amino acids in a region containing a LxxLL-like motif. This suggests that both long-range electrostatic interactions and hydrophobic surfaces may also play a role in stable structure-mediated protein-protein binding.

The binding of TBP to the GR-AF1 (28), ERα-NTD (22), and c-*myc*-transactivation domain (45) increased the level of secondary structure in these proteins. A selective interaction with TBP was identified for the MR-AF1b domain, which was independent of prior induced folding or stabilization of structure. For the MR-AF1b, no dramatic change in secondary structure was observed upon complex formation (Supplemental Fig. 4) or on the solvent exposure of the single tryptophan residue, indicative of local tertiary structure, after treatment with TMAO. In contrast to AR, GR, and ER NTD/AF1 domains, the MR-AF1b showed little propensity to form helical structure. Collectively, our data suggest that the structural basis of MR-AF1b binding to TBP is by a distinct mechanism that does not require induced folding of this region of the MR-NTD. Earlier studies with the yeast activators Gal4 and Gcn4 transactivation domains revealed that they contained significant β-structure and similar to MR-AF1b showed little propensity to form α-helix (46). Taken as whole, the available evidence suggests that, although induced folding and adoption of a more helical structure is a common mechanism for transactivation domains, it is not necessarily a prerequisite for transactivation activity, and other more stable structures can also serve this function. Our data for the MR-NTD transactivation functions illustrate this multiplicity of structure-function relationships within a single transcription factor. The data, together with the previously published studies, also argue for the ability of different secondary structure elements to bind coregulatory proteins and regulate transcription.

A number of investigations of the structure of nuclear receptor NTDs has identified considerable levels of intrinsic disordered structure, which has led to a general model for the conformational plasticity for this domain and the adoption of predominantly α-helical structure upon specific protein-protein interactions (22, 24, 26–28) or phosphorylation (47, 48). The MR-AF1a and MR-MD subdomains clearly fit with this general model, but in contrast, the MR-AF1b appears to exhibit a high degree of structural stability. The concept of intrinsic disorder and its role in protein function has gained wide-spread acceptance in recent years, and the existence of an ensemble of conformations for these regions has been proposed (8, 23, 49–51). A number of advantages has been highlighted for coupling protein folding with protein-protein interactions, including binding specificity without the requirement for high affinity, large interface surface, and the ability to interact with multiple binding partners. More recently, Hilser and Thompson (52) have developed an additional functional model for intrinsic disordered structure involving allosteric coupling and domain-domain interactions. Their model proposes that varying degrees of protein stability and interdomain communication underpin the ensemble of structural conformations, and this primes the system for functional interactions (52). The data presented here for the MR-NTD would be consistent with such a model. In the absence of protein-protein, or DNA interactions or posttranslational modifications, the NTD or regions within this domain exhibit structural plasticity, which undergo induced folding upon

specific interactions. This then creates one or more surfaces that promote further interactions. The evidence from the present study suggests that some regions within the NTD, *e.g.* the MR-AF1b domain, are more stably folded and can interact with protein targets in the absence of induced folding. It is tempting to speculate that the binding of TBP to the AF1b domain may induce structure in other parts of the MR-NTD, analogous to the binding of Jun-dimerization protein 2 to the PR-DBD (24). Further experiments will be required to test this hypothesis.

In conclusion, we have identified structural differences in MR-AF1b domain compared with the GR-AF1 that underpin specific interactions with a common binding partner (TBP), which may also contribute to the selectivity of the MR response in target cells. It will be interesting to investigate the structural consequences of TBP binding for other regions of the MR-NTD and to consider the structural basis of different protein-protein interactions and the impact on receptor action.

Materials and Methods

Plasmid construction

The cDNA for hMR-NTD-DBD was amplified by PCR using the plasmid pRShMR (a gift from Ronald Evans; Salk Institute, San Diego, CA) as a template and the Expand system (Roche, Welwyn Garden City, Hertfordshire, UK). Primers: forward, 5′ GCGCGCAGTTCTACCCCGGCGGAGGCAGGA 3′ and reverse, 5′ GCGCGCAGATCTCCATCActtgtcatcgtcgtccttgtagtc-CTTTCCCAACTTCTTTGACTTTCG 3′; small letters represent the engineered FLAG tag, and the stop codon is underlined. The PCR product was digested with *Bgl*II and cloned into pcDNA3.1 (+) Hygro vector (Invitrogen, Paisley, Scotland, UK) digested with *Bam*HI. Positive clones were identified by restriction enzyme digestion and confirmed by DNA sequencing.

The cDNAs for the isolated hMR-NTD, MR-AF1a, MR-MD, and MR-AF1b domains were amplified by PCR using the plasmid pRShMR as a template and the Expand system (Roche). The sequence of primer pairs for amplification is available on request. The PCR fragments were digested with *Bgl*II and cloned into either pET19bm (53) or pGEX2TK (Amersham Biosciences, Chalfont St Giles, Bucks, UK) at the *Bam*HI cutting site for expression of recombinant His- or GST-tagged MR polypeptides, respectively. Positive clones were confirmed by sequencing and transformed into BL21 (DE3) pLys cells (Novagen, Darmstadt, Germany) for expression of recombinant proteins.

Mutagenesis

Deletion and point mutations of amino acids within the MR-NTD or AF1b region were introduced using double-stranded oligonucleotides and the Quickchange method (Statagen, Workingham, Berkshire, UK). Mutations were screened by restriction endonuclease digestions and the mutation confirmed by DNA sequencing.

Reporter gene assays

COS-1 cells were transfected with wild-type or mutant MR-NTD-DBD expression constructs, together with the $(GRE)_2$-TATA-luciferase reporter gene plasmid, using lipofectamine 2000. After 24 h, cells were harvested, lysed (Promega lysis buffer; Promega, Madison, WI) and luciferase activity measured. The measured relative light units were normalized to total protein recovered (determined by the method of Bradford) and protein expression checked by Western blot analysis using an anti-FLAG antibody (Sigma-Aldrich, Poole, Dorset, UK). In co-transfection experiments, expression plasmids for full-length CBP (0.05 μg pRSV-CBP-HA), SRC2 (0.5 μg pSG5-TIF2), SMRT (0.15 μg pCMX-mSMRTα-FL), and/or empty vector control was included.

Purification of recombinant proteins

Expression of His- or GST-tagged MR polypeptides was induced at OD_{600} 0.4–0.6 by addition of 1 mM isopropyl β-D-thiogalactoside for 3 h and incubation at 37 C or with 0.1 mM isopropyl β-D-thiogalactoside and incubation for 1.5 h at 28 C, respectively. Bacterial cultures [BLR (DE3) cells] were grown in 2xTY media (16 g/liter Bactotryptone, 10 g/liter yeast extract, and 5 g/liter NaCl) containing 0.4 g/liter ampicillin and 0.03 g/liter chloramphenicol. Cell pellets were lysed by freeze thawing and incubation with 0.5 mg/ml lysozyme at 4 C, and recombinant proteins were purified from the soluble (GST-tagged proteins and His-tagged MR-AF1a, MR-MD, and MR-NTD) or insoluble fraction (His-tagged MR-AF1b). Soluble proteins were purified on glutathione-sepharose 4B resin (Amersham Biosciences) or Ni-NTA resin (QIAGEN, Crawley, West Sussex, UK) according to standard procedures, checked by SDS-PAGE for purity, and dialyzed against 25 mM HEPES (pH 7.5), 100 mM sodium acetate, 5% (vol/vol) glycerol, and 1 mM dithiothreitol (protein dialysis buffer). Insoluble proteins were purified under denaturing conditions in urea (54), checked by SDS-PAGE for purity, and dialyzed against protein dialysis buffer containing 1.7 mM SDS during the last steps of dialysis to prevent precipitation.

CD spectroscopy

Purified His-tagged MR-polypeptides were dialyzed against 4 mM NaH_2PO_4, 6 mM Na_2HPO_4, 100 mM $NaSO_4$, 10% (vol/vol) glycerol, and 1 mM dithiothreitol containing 1.7 mM SDS for the AF1b polypeptide. Far-UV CD spectra were measured at 20 C on a Jasco J-810 spectropolarimeter calibrated with (1S)-(+)-10-camphorsulfonic acid. A cell of 0.02-cm path length was used to obtain far-UV spectra (190–260 nm). The far-UV CD spectra for MR-AF1b were also measured in the presence of increasing concentrations of SDS (3.5, 17.3, and 34.7 mM corresponding to 0.1, 0.5, and 1.0%, respectively) and 50% (vol/vol) TFE. The proportions of each secondary structure type were estimated from the CD data using the CDSSTR procedure (55). In each case, the quality of the fitting procedure was judged by the very low value ($\leq$0.03) of the normalized root mean square deviation and the very good superposition of the experimental and reconstructed spectra. Protein concentrations were between 0.07 and 0.2 mg/ml.

Fluorescence spectroscopy

His-tagged MR-AF1a and MR-AF1b polypeptides were analyzed using a Shimadzu 1501 spectrofluorimeter with excitation and emission band widths of 10 nm using a 1-cm path length cuvette. The emission spectra of 0.025 mg/ml protein in

dialysis buffer containing either 6 M urea or 3 M TMAO were measured after excitation at 278 nm.

Partial proteolysis assay

Purified His-tagged MR polypeptides were diluted to a final concentration of 1 μM and digested in proteolysis buffer [25 mM HEPES (pH 7.5), 10% (vol/vol) glycerol, 0.2 mM EDTA, 5 mM $MgCl_2$, 20 mM $CaCl_2$, and 60 mM KCl] at 30 C for varying times with 0.006 g/liter trypsin. Reactions were stopped by the addition of 12.5 μl 4× SDS sample buffer and heating at 75 C for 5 min. Samples were resolved by SDS-PAGE and followed by either silver staining or Western blot analysis with a mouse monoclonal antihexahistidine antibody (Sigma, St. Louis, MO) and detection with enhanced chemiluminescence.

Activity assay of trypsin

The artificial trypsin substrate N-α-benzoyl-L-arginine ethyl ester (0.46 mM) was incubated with 0.012 g/liter trypsin in 63 mM sodium phosphate, 0.06 mM HCl in the presence or absence of SDS. The reactions were monitored at 253 nm, and absorbance readings were taken every 2 min for 45 min.

GST pull-down titration assays

Various concentrations of GST-tagged MR-NTD, MR-AF1a, MR-MD, and MR-AF1b proteins or GST alone were incubated with 25 μl glutathione-sepharose 4B resin (Amersham Biosciences) in 100 μl PBS for 30 min at 4 C, and centrifuged pellets containing bound proteins were resuspended in GST pull-down buffer [20 mM HEPES-KOH (pH7.9), 10% (vol/vol) glycerol, 100 mM NaCl, 5 mM $MgCl_2$, 0.2 mM EDTA, 0.1% (vol/vol) Tween 20, 0.02 g/liter BSA, 1 mM dithiothreitol, and 0.2 mM phenylmethylsulfonylfluoride] in the presence or absence of TMAO and incubated for 30 min at 4 C to allow protein folding. Subsequently, 3–5 μl of ^{35}S labeled prey proteins (Promega TNT Coupled Reticulocyte Lysate System), including CBP (pRSV-CBP-HA), SRC2 (pSG5-TIF2), SRC3 (pCMX-ACTR), RIP140 (pCMV-RIP140), SMRT (pCMX-mSMRTα-FL), or human TBP, were added, incubated for 2 h at 4 C, washed three times in 180 μl GST pull-down buffer, and the centrifuged pellets resuspended in 20 μl of 2× SDS sample buffer. Samples were analyzed by SDS-PAGE followed by phosphoimaging analysis. In the titration pull-down assay, the fraction of CBP or TBP bound was measured and plotted against the concentration of GST or GST-bait proteins. The dissociation constants for the binding of CBP and TBP were calculated from the slope of linear plots of Bound Partner Protein v's Bound Partner/[MR domain] (Eadie-Hofstee plot).

Acknowledgments

We thank Dr. A. Brinkmann (Erasmus University), Dr. P. Chambon (Institut de Génétique et de Biologie Moléculaire et Cellulaire), Dr. R. Evans (Salk Institute), Dr. R. Goodman (Vollum Institute), Dr. R. Kumar (The Commonwealth Medical College), Dr. M. Parker (Imperial College), and Dr. E. B Thompson (University of Texas Medical Branch Galveston) for the kind gift of plasmid reagents used in this study. We also We also thank the UK Biotechnology and Biological Sciences Research Council for support of the Circular Dichroism facility.

Address all correspondence and requests for reprints to: Iain J. McEwan, School of Medical Sciences, University of Aberdeen, Foresterhill, Aberdeen AB25 2ZD, Scotland, United Kingdom. E-mail: iain.mcewan@abdn.ac.uk.

K.F. was supported by a Ph.D. studentship funded by the College of Life Sciences and Medicine and the Development Trust of the University of Aberdeen.

Disclosure Summary: The authors have nothing to disclose.

References

1. **Lifton RP, Gharavi AG, Geller DS** 2001 Molecular mechanisms of human hypertension. Cell 104:545–556
2. **Zennaro MC, Lombès M** 2004 Mineralocorticoid resistance. Trends Endocrinol Metab 15:264–270
3. **Rogerson FM, Brennan FE, Fuller PJ** 2004 Mineralocorticoid receptor binding, structure and function. Mol Cell Endocrinol 217: 203–212
4. **Fuller PJ, Young MJ** 2005 Mechanisms of mineralocorticoid action. Hypertension 46:1227–1235
5. **Viengchareun S, Le Menuet D, Martinerie L, Munier M, Pascual-Le Tallec L, Lombès M** 2007 The mineralocorticoid receptor: insights into its molecular and (patho)physiological biology. Nucl Recept Signal 5:e012
6. **Pippal JB, Fuller PJ** 2008 Structure-function relationships in the mineralocorticoid receptor. J Mol Endocrinol 41:405–413
7. **Thompson EB, Kumar R** 2003 DNA binding of nuclear hormone receptors influences their structure and function. Biochem Biophys Res Commun 306:1–4
8. **Lavery DN, McEwan IJ** 2005 Structure and function of steroid receptor AF1 transactivation domains: induction of active conformations. Biochem J 391:449–464
9. **He B, Gampe Jr RT, Kole AJ, Hnat AT, Stanley TB, An G, Stewart EL, Kalman RI, Minges JT, Wilson EM** 2004 Structural basis for androgen receptor interdomain and coactivator interactions suggests a transition in nuclear receptor activation function dominance. Mol Cell 16:425–438
10. **Arriza JL, Weinberger C, Cerelli G, Glaser TM, Handelin BL, Housman DE, Evans RM** 1987 Cloning of human mineralocorticoid receptor complementary DNA: structural and functional kinship with the glucocorticoid receptor. Science 237:268–275
11. **Pascual-Le Tallec L, Lombès M** 2005 The mineralocorticoid receptor: a journey exploring its diversity and specificity of action. Mol Endocrinol 19:2211–2221
12. **Fuse H, Kitagawa H, Kato S** 2000 Characterization of transactivational property and coactivator mediation of rat mineralocorticoid receptor activation function-1 (AF-1). Mol Endocrinol 14:889–899
13. **Tallec LP, Kirsh O, Lecomte MC, Viengchareun S, Zennaro MC, Dejean A, Lombès M** 2003 Protein inhibitor of activated signal transducer and activator of transcription 1 interacts with the N-terminal domain of mineralocorticoid receptor and represses its transcriptional activity: implication of small ubiquitin-related modifier 1 modification. Mol Endocrinol 17:2529–2542
14. **Govindan MV, Warriar N** 1998 Reconstitution of the N-terminal transcription activation function of human mineralocorticoid receptor in a defective human glucocorticoid receptor. J Biol Chem 273:24439–24447
15. **Fuller PJ, Lim-Tio SS, Brennan FE** 2000 Specificity in mineralocorticoid versus glucocorticoid action. Kidney Int 57:1256–1264
16. **Farman N, Rafestin-Oblin ME** 2001 Multiple aspects of mineralocorticoid selectivity. Am J Physiol Renal Physiol 280:F181–F192
17. **Rupprecht R, Arriza JL, Spengler D, Reul JM, Evans RM, Holsboer F, Damm K** 1993 Transactivation and synergistic properties of the mineralocorticoid receptor: relationship to the glucocorticoid receptor. Mol Endocrinol 7:597–603
18. **Fagart J, Wurtz JM, Souque A, Hellal-Levy C, Moras D, Rafestin-**

Oblin ME 1998 Antagonism in the human mineralocorticoid receptor. EMBO J 17:3317–3325

19. **Bledsoe RK, Madauss KP, Holt JA, Apolito CJ, Lambert MH, Pearce KH, Stanley TB, Stewart EL, Trump RP, Willson TM, Williams SP** 2005 A ligand-mediated hydrogen bond network required for the activation of the mineralocorticoid receptor. J Biol Chem 280:31283–31293
20. **Li Y, Suino K, Daugherty J, Xu HE** 2005 Structural and biochemical mechanisms for the specificity of hormone binding and coactivator assembly by mineralocorticoid receptor. Mol Cell 19:367–380
21. **Kitagawa H, Yanagisawa J, Fuse H, Ogawa S, Yogiashi Y, Okuno A, Nagasawa H, Nakajima T, Matsumoto T, Kato S** 2002 Ligand-selective potentiation of rat mineralocorticoid receptor activation function 1 by a CBP-containing histone acetyltransferase complex. Mol Cell Biol 22:3698–3706
22. **Wärnmark A, Wikström A, Wright AP, Gustafsson JA, Härd T** 2001 The N-terminal regions of estrogen receptor α and β are unstructured in vitro and show different TBP binding properties. J Biol Chem 276:45939–45944
23. **Kumar R, Thompson EB** 2003 Transactivation functions of the N-terminal domains of nuclear hormone receptors: protein folding and coactivator interactions. Mol Endocrinol 17:1–10
24. **Wardell SE, Kwok SC, Sherman L, Hodges RS, Edwards DP** 2005 Regulation of the amino-terminal transcription activation domain of progesterone receptor by a cofactor-induced protein folding mechanism. Mol Cell Biol 25:8792–8808
25. **McEwan IJ, Lavery DN, Fischer K, Watt K** 2007 Natural disordered sequences in the amino terminal domain of nuclear receptors: lessons from the androgen and glucocorticoid receptors. Nuc Rep Sig 5:1–6
26. **Reid J, Kelly SM, Watt K, Price NC, McEwan IJ** 2002 Conformational analysis of the androgen receptor amino-terminal domain involved in transactivation. Influence of structure-stabilizing solutes and protein-protein interactions. J Biol Chem 277:20079–20086
27. **Kumar R, Betney R, Li J, Thompson EB, McEwan IJ** 2004 Induced α-helix structure in AF1 of the androgen receptor upon binding transcription factor TFIIF. Biochemistry 43:3008–3013
28. **Kumar R, Volk DE, Li J, Lee JC, Gorenstein DG, Thompson EB** 2004 TATA box binding protein induces structure in the recombinant glucocorticoid receptor AF1 domain. Proc Natl Acad Sci USA 101:16425–16430
29. **Kumar R, Lee JC, Bolen DW, Thompson EB** 2001 The conformation of the glucocorticoid receptor af1/τ1 domain induced by osmolyte binds co-regulatory proteins. J Biol Chem 276:18146–18152
30. **Wu CS, Ikeda K, Yang JT** 1981 Ordered conformation of polypeptides and proteins in acidic dodecyl sulfate solution. Biochemistry 20:566–570
31. **Zhong L, Johnson Jr WC** 1992 Environment affects amino acid preference for secondary structure. Proc Natl Acad Sci USA 89:4462–4465
32. **Eftink MR, Ghiron CA** 1976 Exposure of tryptophanyl residues in proteins. Quantitative determination by fluorescence quenching studies. Biochemistry 15:672–680
33. **Baskakov I, Bolen DW** 1998 Forcing thermodynamically unfolded proteins to fold. J Biol Chem 273:4831–4834
34. **Kumar R, Serrette JM, Thompson EB** 2005 Osmolyte-induced folding enhances tryptic enzyme activity. Arch Biochem Biophys 436:78–82
35. **Dahlman-Wright K, Baumann H, McEwan IJ, Almlöf T, Wright AP, Gustafsson JA, Härd T** 1995 Structural characterization of a minimal functional transactivation domain from the human glucocorticoid receptor. Proc Natl Acad Sci USA 92:1699–1703
36. **Heery DM, Kalkhoven E, Hoare S, Parker MG** 1997 A signature motif in transcriptional co-activators mediates binding to nuclear receptors. Nature 387:733–736
37. **Meijer OC, Kalkhoven E, van der Laan S, Steenbergen PJ, Houtman SH, Dijkmans TF, Pearce D, de Kloet ER** 2005 Steroid receptor coactivator-1 splice variants differentially affect corticosteroid receptor signaling. Endocrinology 146:1438–1448
38. **Obradović D, Tirard M, Némethy Z, Hirsch O, Gronemeyer H, Almeida OF** 2004 DAXX, FLASH, and FAF-1 modulate mineralocorticoid and glucocorticoid receptor-mediated transcription in hippocampal cells–toward a basis for the opposite actions elicited by two nuclear receptors? Mol Pharmacol 65:761–769
39. **Yokota K, Shibata H, Kurihara I, Kobayashi S, Suda N, Murai-Takeda A, Saito I, Kitagawa H, Kato S, Saruta T, Itoh H** 2007 Coactivation of the N-terminal transactivation of mineralocorticoid receptor by Ubc9. J Biol Chem 282:1998–2010
40. **Pascual-Le Tallec L, Simone F, Viengchareun S, Meduri G, Thirman MJ, Lombès M** 2005 The elongation factor ELL (eleven-nineteen lysine-rich leukemia) is a selective coregulator for steroid receptor functions. Mol Endocrinol 19:1158–1169
41. **Copik AJ, Webb MS, Miller AL, Wang Y, Kumar R, Thompson EB** 2006 Activation function 1 of glucocorticoid receptor binds TATA-binding protein *in vitro* and *in vivo*. Mol Endocrinol 20:1218–1230
42. **Wu Y, Reece RJ, Ptashne M** 1996 Quantitation of putative activator-target affinities predicts transcriptional activating potentials. EMBO J 15:3951–3963
43. **Hermann S, Berndt KD, Wright AP** 2001 How transcriptional activators bind target proteins. J Biol Chem 276:40127–40132
44. **Ferreira ME, Hermann S, Prochasson P, Workman JL, Berndt KD, Wright AP** 2005 Mechanism of transcription factor recruitment by acidic activators. J Biol Chem 280:21779–21784
45. **McEwan IJ, Dahlman-Wright K, Ford J, Wright AP** 1996 Functional interaction of the c-Myc transactivation domain with the TATA binding protein: evidence for an induced fit model of transactivation domain folding. Biochemistry 35:9584–9593
46. **Van Hoy M, Leuther KK, Kodadek T, Johnston SA** 1993 The acidic activation domains of the GCN4 and GAL4 proteins are not α helical but form β sheets. Cell 72:587–594
47. **Chen W, Dang T, Blind RD, Wang Z, Cavasotto CN, Hittelman AB, Rogatsky I, Logan SK, Garabedian MJ** 2008 Glucocorticoid receptor phosphorylation differentially affects target gene expression. Mol Endocrinol 22:1754–1766
48. **Garza AM, Khan SH, Kumar R** 2010 Site-specific phosphorylation induces functionally active conformation in the intrinsically disordered N-terminal activation function (AF1) domain of the glucocorticoid receptor. Mol Cell Biol 30:220–230
49. **Tompa P** 2005 The interplay between structure and function in intrinsically unstructured proteins. FEBS Lett 579:3346–3354
50. **Liu J, Perumal NB, Oldfield CJ, Su EW, Uversky VN, Dunker AK** 2006 Intrinsic disorder in transcription factors. Biochemistry 45:6873–6888
51. **Fuxreiter M, Tompa P, Simon I, Uversky VN, Hansen JC, Asturias FJ** 2008 Malleable machines take shape in eukaryotic transcriptional regulation. Nat Chem Biol 4:728–737
52. **Hilser VJ, Thompson EB** 2007 Intrinsic disorder as a mechanism to optimize allosteric coupling in proteins. Proc Natl Acad Sci USA 104:8311–8315
53. **Rowlands JC, McEwan IJ, Gustafsson JA** 1996 Trans-activation by the human aryl hydrocarbon receptor and aryl hydrocarbon receptor nuclear translocator proteins: direct interactions with basal transcription factors. Mol Pharmacol 50:538–548
54. **Watt K, Jess TJ, Kelly SM, Price NC, McEwan IJ** 2005 Induced α-helix structure in the aryl hydrocarbon receptor transactivation domain modulates protein-protein interactions. Biochemistry 44:734–743
55. **Sreerama N, Woody RW** 1993 A self-consistent method for the analysis of protein secondary structure from circular dichroism. Anal Biochem 209:32–44
56. **Li X, Romero P, Rani M, Dunker AK, Obradovic Z** 1999 Predicting protein disorder for N-, C-, and internal regions. Genome Inform Ser Workshop Genome Inform 10:30–40
57. **Oldfield CJ, Cheng Y, Cortese MS, Brown CJ, Uversky VN, Dunker AK** 2005 Comparing and combining predictors of mostly disordered proteins. Biochemistry 44:1989–2000
58. **Combet C, Blanchet C, Geourjon C, Deléage G** 2000 NPS@: network protein sequence analysis. Trends Biochem Sci 25:147–150